Journal of Hydrology 536 (2016) 208–221

Contents lists available at ScienceDirect

Journal of Hydrology

journal homepage: www.elsevier.com/locate/jhydrol

Precipitation and temperature changes in the major Chinese river basins during 1957–2013 and links to sea surface temperature

Qing Tian [a,*], Matthias Prange [b], Ute Merkel [b]

[a] State Key Laboratory of Estuarine and Coastal Research, East China Normal University, 200062 Shanghai, China
[b] MARUM – Center for Marine Environmental Sciences, Department of Geosciences, University of Bremen, D-28334 Bremen, Germany

ARTICLE INFO

Article history:
Received 19 October 2015
Received in revised form 28 January 2016
Accepted 27 February 2016
Available online 3 March 2016
This manuscript was handled by Konstantine P. Georgakakos, Editor-in-Chief, with the assistance of Marco Borga, Associate Editor

Keywords:
Chinese rivers
Precipitation
Temperature
SST
Mann–Kendall test
MCA

SUMMARY

The variation characteristics of precipitation and temperature in the three major Chinese river basins (Yellow River, Yangtze River and Pearl River) in the period of 1957–2013 were analyzed on an annual and seasonal basis, as well as their links to sea surface temperature (SST) variations in the tropical Pacific and Indian Ocean on both interannual and decadal time scales. Annual mean temperature of the three river basins increased significantly overall since 1957, with an average warming rate of about 0.19 °C/10a, but the warming was characterized by a staircase form with steps around 1987 and 1998. The significant increase of annual mean temperature could mostly be attributed to the remarkable warming trend in spring, autumn and winter. Warming rates in the northern basins were generally much higher than in the southern basins. However, both the annual precipitation and seasonal mean precipitation of the three river basins showed little change in the study area average, but distinct interannual variations since 1957 and clear regional differences. An overall warming–wetting tendency was found in the northwestern and southeastern river basins in 1957–2013, while the central regions tended to become warmer and drier.

Results from a Maximum Covariance Analysis (MCA) showed that the interannual variations of seasonal mean precipitation and surface air temperature over the three river basins were both associated with the El Niño-Southern Oscillation (ENSO) since 1957. ENSO SST patterns affected precipitation and surface air temperature variability throughout the year, but with very different response patterns in the different seasons. For instance, temperature in most of the river basins was positively correlated with central-eastern equatorial Pacific SST in winter and spring, but negatively correlated in summer and autumn. On the decadal time scale, the seasonal mean precipitation and surface air temperature variations were strongly associated with the Pacific Quasi-Decadal Oscillation.

1. Introduction

Rivers are the major pathways for the delivery of freshwater and terrestrial material to the ocean (Walling and Fang, 2003; Meybeck and Vörösmarty, 2005). Riverine discharges greatly affect the geomorphic evolution, the ecological environment, the construction and maintenance of hydraulic engineering, as well as the economic development in both the drainage basins and the coastal zones (Lamberth et al., 2009; Wang et al., 2010; Hoan et al., 2011; Park et al., 2011; Dai et al., 2014; Yang et al., 2014). Consequently, timely monitoring and research on riverine discharges is of great practical importance.

Most Chinese river basins are located in the East Asian monsoon region, one of the major monsoonal regions in the world. Under the alternating influence of winter and summer monsoon, the river basins exhibit a distinct annual cycle of dry and rainy seasons. Of all the Chinese rivers, the Yellow River, the Yangtze River and the Pearl River are the top three largest from north to south respectively, and hundreds of tributaries developed a lot of sub-basins in the three river basins (Fig. 1). The total drainage area of the three rivers is 3×10^6 km^2 (Table 1), which accounts for about 1/3 of the Chinese territory. They roughly run from the western mountainous area to the eastern plain, and finally discharge into the Western Pacific Ocean by way of the Bohai and Yellow Sea, the East China Sea and the South China Sea, from north to south respectively (Fig. 1). Both the Yellow River and the Yangtze River originate from the permanently snow-covered Qinghai–Tibet Plateau in West China, which has been known as 'the roof of the world', while

* Corresponding author at: State Key Laboratory of Estuarine and Coastal Research, East China Normal University, 3663 N. Zhongshan Rd., Shanghai 200062, China.
E-mail address: tianqing0405@hotmail.com (Q. Tian).

http://dx.doi.org/10.1016/j.jhydrol.2016.02.048
0022-1694/

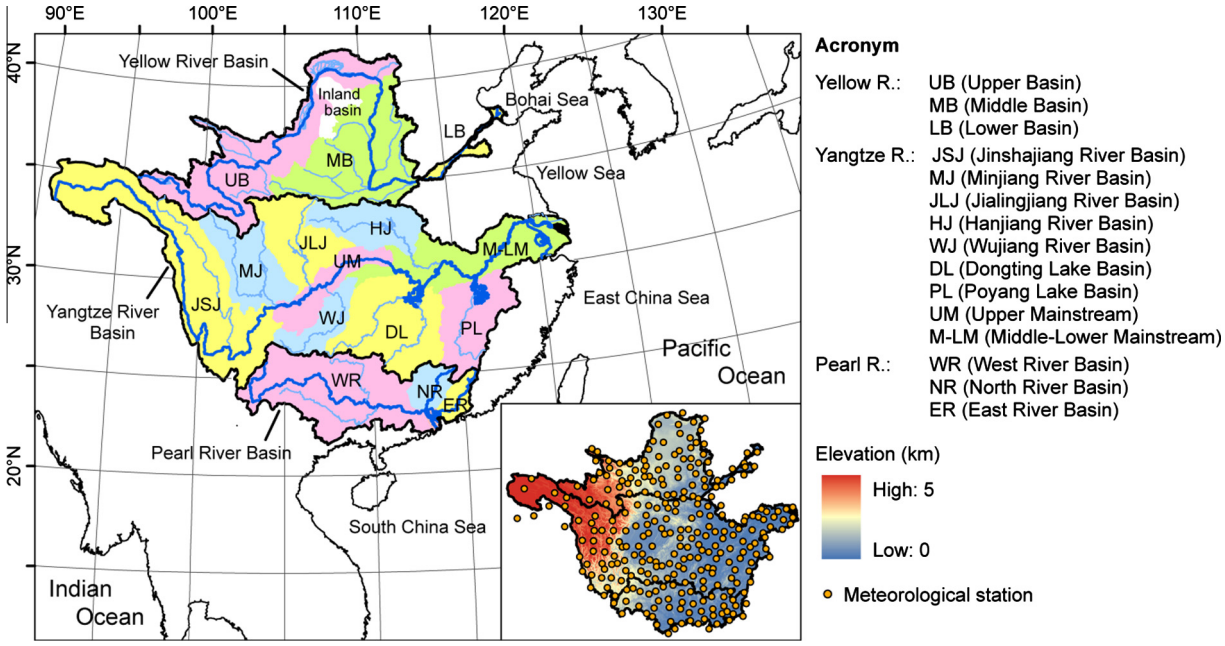

Fig. 1. Location of the three river basins and meteorological stations.

Table 1
Basic data of the three rivers.

Rivers	Yellow River	Yangtze River	Pearl River
Headstream	Tibetan Plateau	Tibetan Plateau	Yungui Plateau
Basin area (10^3 km^2)	753	1800	442
River length (10^3 km)	5.46	6.30	2.21
Runoff (10^9 m^3/a)	30	896	283
Sediment load (10^9 kg/a)	722	390	72
Average population density (people/km^2)	143	220	203

Data source: The website of the Ministry of Water Resources of China (http://www.mwr.gov.cn/); runoff and sediment load data (1950s–2010) are from the Chinese River Sediment Bulletin (2013).

the Pearl River originates from the Yungui Plateau in Southwest China. The water and sediment yields in the Chinese river basins are determined by a lot of factors. As numerous studies reported, human activities, like water diversion, water and soil conservation measures and dam constructions, were mainly responsible for the drastic long-term decline of river discharge since the 1950s (H. Wang et al., 2011). Climate variability, in particular on interannual time scales, was also very important for the hydrological cycle in the river basins due to the sensitive and immediate response of hydrological processes (Liu et al., 2010, 2012). Precipitation is usually the major water source in the river basins, and dominates the runoff. According to Lu (2004), on average about half of the annual precipitation could be transformed into runoff in Chinese river systems, slightly higher than the global average value of 40% (Gerten et al., 2008). Precipitation changes might lead to augmented changes in runoff and subsequent changes in sediment, especially for rivers with little recharge from glacier melt water (Legesse et al., 2010; Shi et al., 2012). Gerten et al. (2008) reported that the increase by 7.7% in global river discharge over 1901–2002 was primarily related to the concurrent global precipitation increase by 2.5%. The runoff response to the increase in evaporation due to rising temperatures may be much slower than to the variation in precipitation (Wagener et al., 2005; Dai et al., 2009). Increasing temperature might also intensify the local precipitation by altering the thermo-dynamic properties of air masses and the moisture transport (Gardner, 2009; Zhou and Huang, 2010; Trenberth et al., 2011), thus exerting both a direct and an indirect influence on runoff.

Regionally, the hydrological responses to climate anomalies showed different characteristics depending on locations and seasons. For example, runoff anomalies in humid areas were more related to precipitation, but more sensitive to evapotranspiration in arid regions (Liu and Cui, 2011). Climate change in humid areas might induce a higher and more variable runoff than in arid areas (Shi et al., 2012). It also should be noted that the hydrological and ecological environments in the arid and semi-arid river basins are very fragile and more vulnerable to climate change than in humid basins (Lu, 2004). River courses shortened, and inland lakes contracted or even dried up due to warming in arid regions (Wang and Cheng, 2000). In contrast, the water-levels in closed lakes recharged by glacier water rose in response to climate warming (Song et al., 2014). The contribution of climate change to the variation of hydrological elements was possibly much higher in plain river basins located in low latitudes with little recharge by glacier melt water. Therefore, studies on the temporal variability of temperature and precipitation are of great importance to the water resource management in the river basins.

The climate and environmental backgrounds, as well as the socio-economic development differ a lot among the three major Chinese river basins (Table 1). Therefore, it is necessary to perform comparative studies to disentangle climate variations in the river basins, especially in the period since the 1950s, which has experienced the most obvious global climate change during the last 150 years (IPCC AR5, 2013). Previous studies have analyzed the temperature and precipitation changes in China, but were focused on different periods, spatial scales, indices or methods (e.g. Hu et al., 2003; Zhai et al., 2005; Wang et al., 2014; Yu et al., 2014; Liang et al., 2015). For example, the climate variations in a single river basin were analyzed in previous papers (e.g. Xu et al., 2006; Liu and Cui, 2011; Y. Wang et al., 2011; Wu et al., 2012; Cuo et al., 2013; Sun et al., 2013), but a comprehensive comparative study of climate variations in the major Chinese river basins has not been performed. Moreover, updated data are used in our study,

which is important for a meaningful assessment of hydrometeorological time series based on observations.

Furthermore, changes in global sea surface temperature (SST) patterns and large scale atmospheric circulation have been shown to be associated with regional changes in temperature and precipitation extremes due to teleconnections (Alexander et al., 2009; Kenyon and Hegerl, 2010; Li et al., 2012), particularly in regions around the Pacific rim (Kenyon and Hegerl, 2008). Previous studies using coupled ocean–atmosphere circulation models have significantly enhanced our knowledge of the physical teleconnection mechanisms responsible for monsoon changes associated with SST anomalies. For example, Wang et al. (2000) explained the ENSO effect on East Asian climate by emphasizing the importance of air–sea interaction over the Philippine Sea in modulating the strength and location of the western North Pacific anticyclone. Li et al. (2010) showed that especially the warming associated with the tropical interdecadal variability centered over the central and eastern Pacific, is a primary cause for the weakening of the East Asian summer monsoon since the late 1970s. In general, monsoon–ENSO relationships are closely tied to the large-scale Walker circulation (e.g. Kumar et al., 2006; Miyakoda et al., 2007). Existing studies on the coupling of climate variations over China to SST of the adjacent oceans using observational data, however, mainly discussed the links of changes in SST and precipitation on the annual scale (e.g. Wang et al., 2014), or in the rainy season (e.g. Lau and Wu, 2001; Yang and Lau, 2004; Hartmann et al., 2008; Ye, 2014), or in the perspective of extreme precipitation events (e.g. Wang et al., 2014). By contrast, little attention was paid to other seasons. However, especially in the southern river basins with a longer rainy season, other seasons than summer may also contribute to annual precipitation variability, in particular since eastern tropical Pacific SST anomalies usually peak in winter. Besides, the links of seasonal air temperature over China and SST in the tropical oceans, to our knowledge, have been given little consideration in the literature so far. All of this provided a great motivation to study comprehensively the coupling also separately for the different river basins and in different seasons.

In our study, temporal variations in precipitation and temperature both annually and seasonally in the three major Chinese river basins in 1957–2013 were analyzed to explore the long-term and interannual climate characteristics over these basins, and a regional synthesis was made. In addition, the covariance of the seasonal mean precipitation and temperature fields in the three river basins with SST in the Pacific and Indian Oceans, which can be considered as one of the most important driving factors of the regional atmospheric circulation and the hydrological cycle, was also investigated in this study.

2. Data and methodology

2.1. Data

The monthly precipitation and temperature data for 1957–2013 were selected from 290 meteorological stations that were almost evenly distributed within and surrounding the study area (Fig. 1). The meteorological data were provided by the National Meteorological Information Center (NMIC) of the China Meteorological Administration and were available at http://data.cma.gov.cn/. This is one of the best meteorological datasets available for China and has been subject to strict quality control by NMIC (Zhai et al., 2005; Wang et al., 2014; Yu et al., 2014; Liang et al., 2015), including the identification of outliers, internal consistency check, spatial and temporal consistency checks, and correction of suspected and erroneous data (Liu and Ren, 2005). Besides, Ma et al. (2015) have shown that the NMIC dataset of daily precipitation is sufficiently homogeneous, with significant change points and discontinuities only at a small fraction (~5%) of the stations, and the discontinuities do not have a significant impact on national and regional averages. This assessment provides much confidence to the NMIC dataset used in this study to document the long-term temperature and precipitation changes over the study area. Several stations have some missing data records in the early time (1957–1960) of the study period, such that about 0.38% of all the monthly precipitation (or temperature) data are missing. The gaps of precipitation data were filled by the spatially interpolated data calculated by the ordinary Kriging method (Krige, 1951; Matheron, 1973), while missing temperature data at a certain station were filled using linear regression to well correlated neighboring stations.

SST data were provided by the Met Office Hadley Centre, UK (Rayner et al., 2003). In our study, the SST data for the region of 60°E–60°W, 50°N–30°S were considered, with a resolution of $1° \times 1°$ (available at http://www.metoffice.gov.uk/hadobs/hadisst/data/download.html). The time series of global average temperature over land (Jones et al., 2012) was available at http://www.metoffice.gov.uk/hadobs/crutem4/index.html.

2.2. Methodology

We used the nonparametric Mann–Kendall (MK) test (Mann, 1945; Kendall, 1975) to identify monotonic trends in the meteorological time series. The MK test does not require the data to be normally distributed and has low sensitivity to outliers or abrupt breaks in the time series, and thus it has been widely used for the trend analysis of climatological–hydrological time series (K.H. Xu et al., 2010; Fu et al., 2013). This method assumes that the analyzed data points are independent and randomly ordered, and tests the null hypothesis H_0 that there is no significant trend. It contains two parameters: Z_{mk} and β. Z_{mk} reflects the general trend of the series with positive (negative) values denoting an overall upward (downward) trend. If $|Z_{mk}| > 1.96$ (the critical value at the 95% confidence level according to the standard normal distribution function), H_0 will be rejected, which means there is a statistically significant trend in the series, otherwise it will be accepted (no significant trend). The parameter β provides an estimate of the average rate of change within the time series.

Transition or break points in the time series were detected using Accumulated Anomaly Curves (Hao et al., 2008). This method is useful for time series that do not exhibit a constant trend throughout the length of the time series. The accumulated anomaly of a time series $(x_1, x_2, \ldots, x_n)$, e.g. temperature at a specific geographical location, is defined as:

$$X_t = \sum_{i=1}^{t} (x_i - \bar{x}) \quad (t = 1, 2, \ldots, n)$$

with $\bar{x} = \frac{1}{n}\sum_{i=1}^{n} x_i$. An upward trend of the curve indicates a relatively warm or pluvial period, whereas a downward trend denotes a cold or dry period. Thus, a transition point of the curve may be interpreted as a change of regime.

Maximum Covariance Analysis (MCA) was then applied to detect spatiotemporal coupled modes of surface air temperature/precipitation in our study area and SST on both the interannual and decadal time scales, based on the 7-year high-pass and 7–15 year band-pass filtered detrended data, respectively. MCA is also referred to as the Singular Value Decomposition (SVD) method, because it is based on the decomposition of a "cross-covariance matrix" derived from the two data fields analyzed jointly (Bretherton et al., 1992; Wallace et al., 1992). It should be pointed out that the coupled patterns may a priori have no physical meaning (Yang and Lau, 2004), and possible lead-lag relationships have not been considered in our study. The advantage of this

technique is to identify covariations between two fields of variables, specifically how the SSTs over different ocean regions may be coupled to temperature (precipitation) over our study area, without pre-defining the potentially contributing ocean regions.

Besides, the homogeneous and heterogeneous correlation maps (Bretherton et al., 1992; Wallace et al., 1992; Kam et al., 2014), which depict the temporal correlations between the leading SVD mode of SST and gridded SSTs (homogeneous correlation) and between the leading SVD mode of SST and station precipitation/land temperature (heterogeneous correlation), respectively, were calculated to examine to which extent the precipitation/land temperature variations can be explained by or predicted from the SST variations of the leading mode.

Z_{mk} and β results from the MK test and the homogeneous/heterogeneous correlation coefficients from the MCA were spatially interpolated by the ordinary Kriging interpolation method.

3. Results

3.1. Long-term mean climate of the study area

The multi-year averages of annual mean temperature and annual precipitation averaged over the whole study area were about 12.04 °C and 926.49 mm respectively in 1957–2013 (Table 2). However, annual mean temperature and annual precipitation showed a clear gradient across the three river basins in southeast–northwestern direction. In particular, temperature disparities between the northwestern and southeastern parts of our study area were about 25 °C with lowest temperatures in the northwest (Fig. 2A). Annual precipitation showed differences of about 1600 mm between the wet southeastern and the dryer northwestern part (Fig. 2B). Consequently, the southeast river basin showed warm and humid conditions, while it was cold and dry in the northwestern basin, mainly due to the distance to the sea, the latitude and the topography.

On the basin scale, there were differences of about 6–7 °C in annual mean temperature and 400–600 mm in annual precipitation on average between neighboring river basins (Table 2).

3.2. Temporal variations over the three river basins in 1957–2013

3.2.1. Annual mean temperature and annual precipitation

Since 1957, the annual mean temperature of the three river basins has increased significantly at the 95% confidence level according to the MK test (Table 2). The average warming rate (β) in the study area was about 0.19 °C/10a (Figs. 3A and 4, Table 2). The significant warming over the three river basins was characterized by a staircase form instead of a monotonic upward trend over the past 57 years, with significant warming transitions around 1987 and 1998, respectively, shown by the Accumulated Anomaly Curves of annual mean temperature (Fig. 5B). Average annual mean temperatures after 1998 were about 1.20, 0.83 and 0.58 °C higher than those before 1987 in the Yellow River, Yangtze River and Pearl River basins, respectively (Table 3). The observed pronounced warming after 1987 in the study area shows similarities to the global warming since around 1979 (IPCC AR5, p. 187), but with the warming setting in about 8 years later (Fig. 4). A switch from solar dimming to solar brightening around 1990 might have partly contributed to this temperature evolution in China (e.g. Ye et al., 2010).

However, in contrast to the annual mean temperature trends during the past 57 years, the annual precipitation over the three river basins did neither exhibit a significant trend (Table 2) nor any obvious periodical fluctuations or transition points based on the Accumulated Anomaly Curve (not shown). Annual precipitation showed distinct interannual variations (Fig. 6), especially in the southern basins, and caused extremely wet years, notably 1964 in the Yellow River Basin, 1998 in the Yangtze River Basin and 1994 in the Pearl River Basin, as well as drought years, like 1965 in the Yellow River Basin and 2011 in the Yangtze River and the Pearl River basins. The standard deviations of annual precipitation in the three river basins were 59.21, 73.72 and 163.12 mm respectively from north to south.

3.2.2. Seasonal mean temperature and precipitation

Since the three river basins are located in the typical East Asian monsoon area, the climate conditions there show strong seasonality (Fig. 7), with about half of the annual precipitation concentrated in the summer season in most of the study area, but MAM (March–April–May) and SON (September–October–November) also make large contributions (Fig. 7), e.g. up to 40% during MAM in the southeast (e.g. the Pearl River Basin), due to the earlier onset of the monsoon season (Fig. 7A) or up to 30% in the central part during SON (Fig. 7C).

The temperature change since 1957 showed strong seasonality: The temperature exhibited warming trends in all seasons (Fig. 8), but a significant warming over the whole study area was only found in autumn (Fig. 8C). On the river basin scale, the Yellow River Basin warmed remarkably all year round. A weaker but significant warming in the Pearl River Basin only occurred in summer and autumn, while the Yangtze River Basin showed very heterogeneous seasonal warming trends. Consequently, the increase of annual mean temperature in the three river basins was mainly attributable to the significant warming in autumn (Fig. 8C) and even more in winter (Fig. 8D), particularly in the Yellow River Basin and the source region of the Yangtze River Basin. These results support the conclusion of previous research that the warming in China mainly occurred in autumn and winter (Ren et al., 2011), reflected by a remarkable increase in the minimum temperature (Zhang et al., 2013). For the summer season, a small part of the Yangtze River Basin showed a cooling trend (albeit not statistically significant, Fig. 8B), while previous studies showed a more pronounced cooling over the basin region based on shorter time series (e.g. Ye, 2014). Moreover, the Accumulated Anomaly Curves of seasonal mean temperature suggest step-like changes, but with different transition points in the 1980s–1990s for the different seasons and river basins (Fig. 9).

The seasonal mean precipitation hardly changed overall over the whole study area since 1957, and statistically significant trends

Table 2
MK test results of annual mean temperature and annual precipitation trends in the three river basins. The H_0 columns denote acceptance (A) or rejection (R) of the null hypothesis H_0.

1957–2013	Annual mean temperature				Annual precipitation			
	Multiyear average (°C)	Z_{mk}	β (°C/10a)	H_0	Multiyear average (mm)	Z_{mk}	β (mm/10a)	H_0
Yellow River	6.92	5.76	0.27	R	454.34	−0.81	−3.62	A
Yangtze River	12.94	4.74	0.17	R	1042.19	−0.41	−2.33	A
Pearl River	19.38	3.68	0.11	R	1462.20	−0.57	−8.99	A
Entire three basins	12.04	5.14	0.19	R	926.49	−0.89	−2.70	A

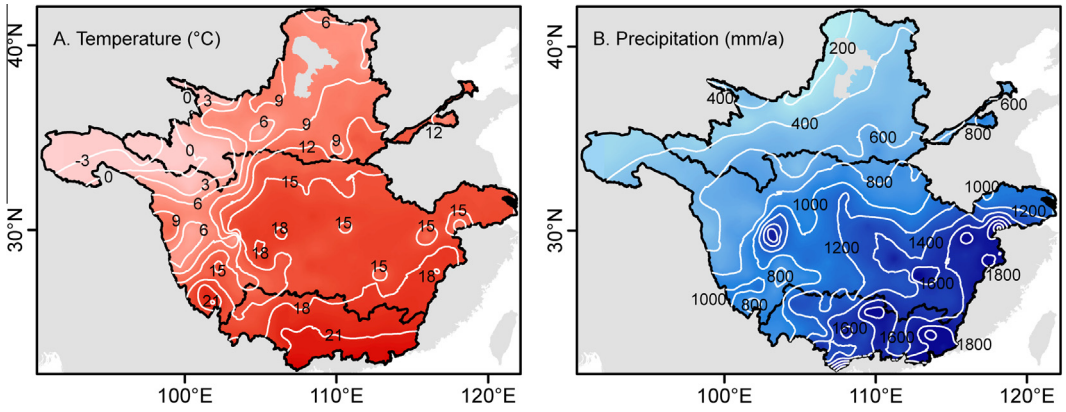

Fig. 2. Multi-year average of annual mean temperature (A) and annual precipitation (B) in 1957–2013.

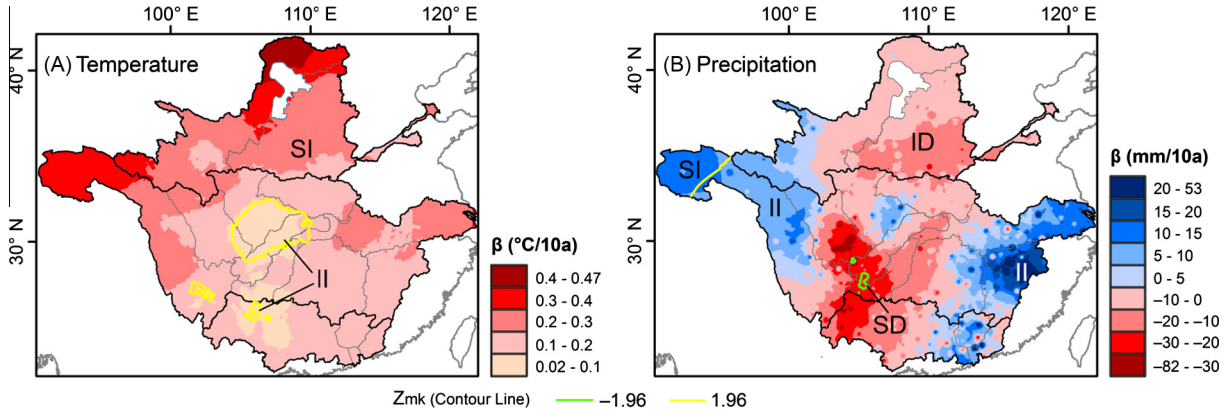

Fig. 3. (A) Average warming rate [°C/10a] and (B) average precipitation change [mm/10a] during 1957–2013 according to the Mann–Kendall test. Green and yellow lines denote the Z_{mk} critical values. SI: Significant increase; II: insignificant increase; SD: significant decrease; ID: insignificant decrease (see text for details). (For interpretation of the references to color in this figure legend, the reader is referred to the web version of this article.)

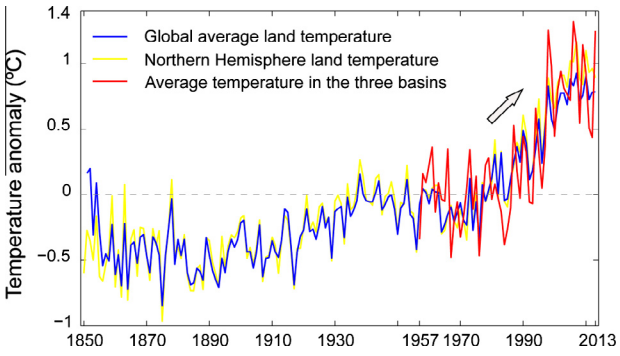

Fig. 4. Anomalies of annual mean temperature averaged over the three river basins (red line), global average land temperature (blue line) and northern hemisphere land temperature (yellow line) are given with respect to the 1961–1990 base period. (For interpretation of the references to color in this figure legend, the reader is referred to the web version of this article.)

of increasing seasonal mean precipitation were only found in parts of the source region of the Yangtze River in spring (Fig. 8E), as well as in a small part of the Lower Basin of the Yangtze River in summer (Fig. 8F) and winter (Fig. 8H). It should be noted that seasonal mean precipitation displayed spatially heterogeneous changes. The trend pattern of summer precipitation resembles that of annual precipitation (Fig. 3B), and the largest magnitude of change occurred in summer associated with the East Asian summer monsoon. As annual precipitation, the Accumulated Anomaly Curves of seasonal mean precipitation also showed no systematic characteristics/transition points, except in the autumn season, where they all indicated a decreasing tendency of precipitation in the late 1980s (not shown).

3.2.3. Inter-basin comparison of trends

Statistically significant upward trends in temperature were observed over almost the whole study area since 1957 (Fig. 3A). The warming over the study area corresponded well with the global trend, but with much higher magnitude over the same period (Fig. 4). However, warming rates showed substantial regional differences (Fig. 3A): the highest warming was found in the Yellow River Basin and the western source region of the Yangtze River on the Qinghai–Tibetan Plateau, as well as in the eastern coastal area of the Yangtze River Basin with flat topography and intense human activities. The average warming rates of annual mean temperature in the three river basins were 0.11, 0.17 and 0.27 °C/10a (Table 2), which indicated a total increase of 0.62, 0.95 and 1.51 °C respectively from south to north for the last 57 years. Evidently, the warming rates in the northern basins were much higher than that in the southern basins in the period of 1957–2013. The warming rate of the global average land-surface air temperature was 0.18 ± 0.04 °C/10a in 1951–2012, with the highest warming rate of around 0.25 ± 0.05 °C/10a since 1979 (IPCC AR5, 2013). Thus, the average warming rate since 1957 in the Yangtze River Basin was comparable to the global average value, but lower in the Pearl River Basin. In contrast, it was much higher than the

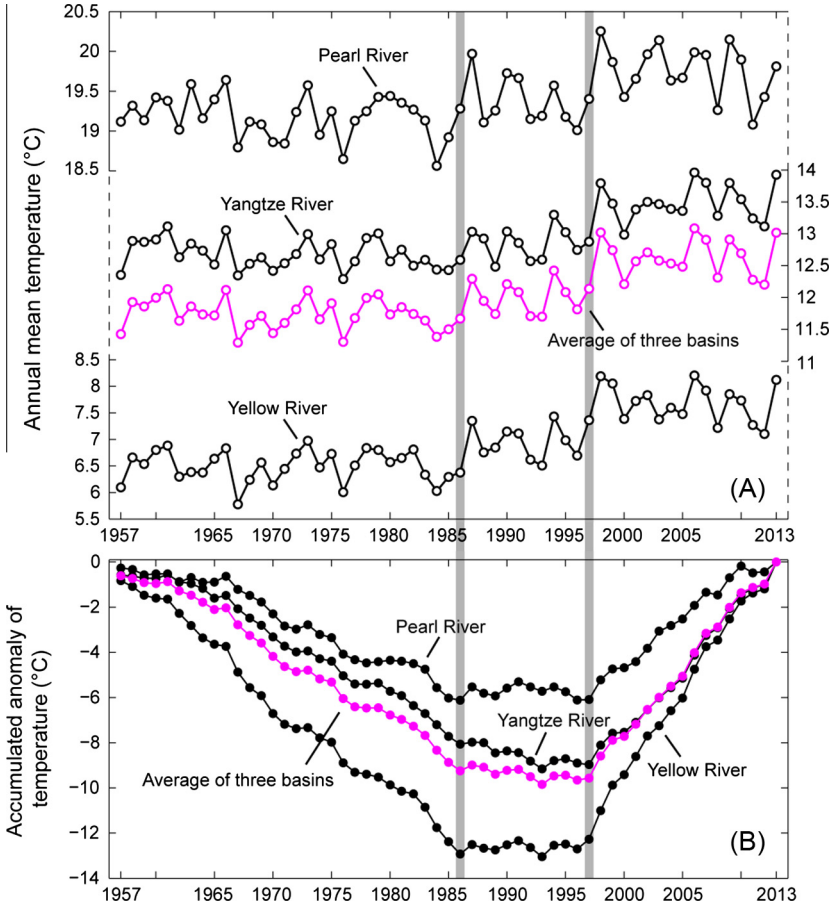

Fig. 5. Annual mean temperature (A) and its Accumulated Anomaly Curve (B) for each of the three river basins. The average over all three basins is denoted by the pink line. The gray bars denote the transitions of the trends according to the Accumulated Anomaly Curve (B). (For interpretation of the references to color in this figure legend, the reader is referred to the web version of this article.)

Table 3
Annual mean temperature in the time intervals marked by the gray bars in Fig. 5 and difference between the first and last intervals.

Annual mean temperature (°C)	1957–1986	1987–1997	1998–2013	(1998–2013)–(1957–1986)
Yellow River	6.49	6.98	7.69	1.20
Yangtze River	12.67	12.86	13.50	0.83
Pearl River	19.18	19.38	19.76	0.58
Entire three basins	11.73	12.01	12.64	0.91

global average in the Yellow River Basin, and even close to the highest global warming rate since 1979.

A slight (albeit not statistically significant) decrease of annual precipitation was detected in the whole study area (Table 2). However, similar to our findings for temperature, the precipitation trends showed regional differences (Fig. 3B). A general decrease was found mostly in the central part of the study area (the Middle–Lower basins of the Yellow River, the central area of the Yangtze River and the West River Basin of the Pearl River), in

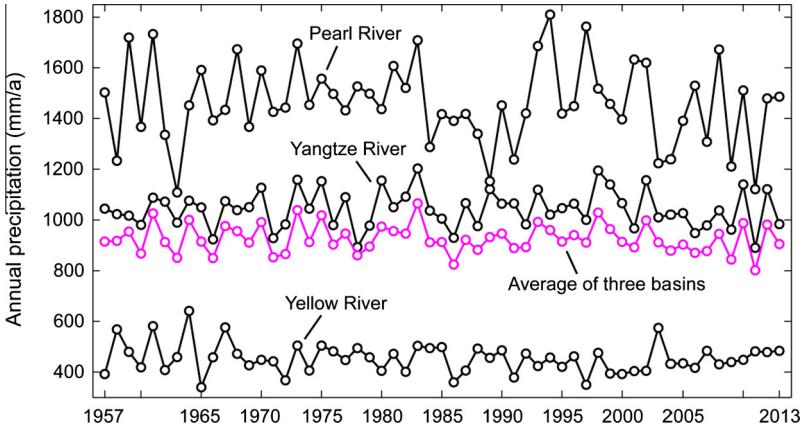

Fig. 6. Annual precipitation in the Yellow, Yangtze and Pearl River basins (1957–2013). The average over all three basins is denoted by the pink line. (For interpretation of the references to color in this figure legend, the reader is referred to the web version of this article.)

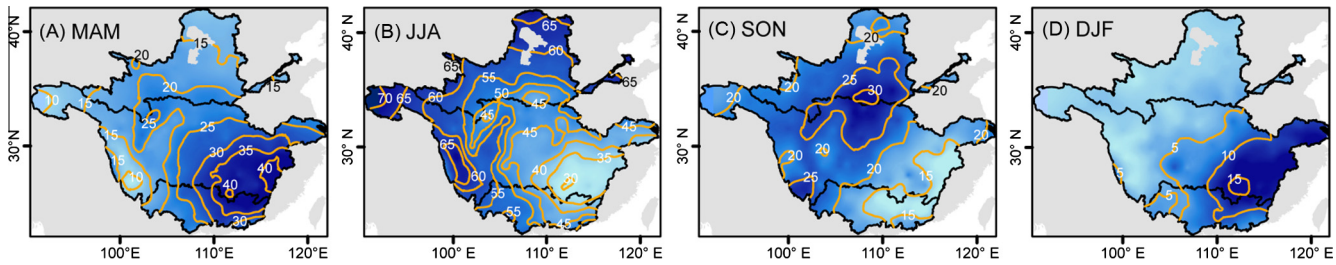

Fig. 7. Ratio of seasonal precipitation (seasonal sum) to the annual precipitation (given in %) for the four seasons of (A) March–May, (B) June–August, (C) September–November, and (D) December–February.

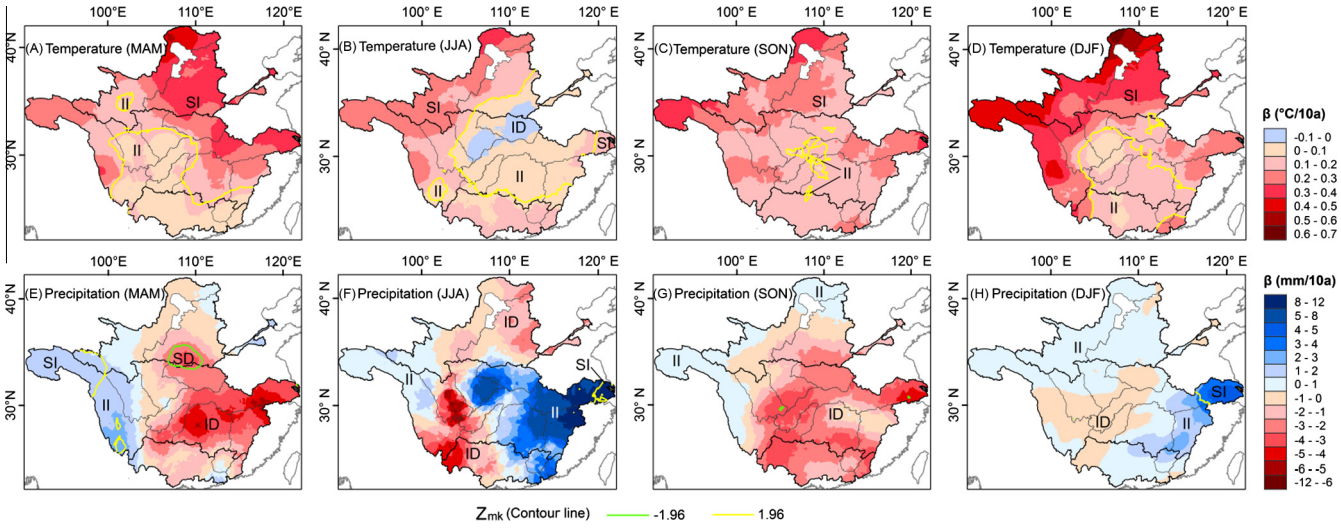

Fig. 8. As Fig. 3, but for seasonal mean temperature (A–D) and precipitation (E–H).

contrast to a slight increase in the source regions of the Yellow River and the Yangtze River on the Qinghai–Tibetan Plateau, as well as in the Middle–Lower basins in the southeastern river basin. Zhang et al. (2013) and Zhai et al. (2005) reported a similar wetting tendency in Western China, including some western inland river basins, like the Tarim River Basin in Xinjiang Province (Hao et al., 2008; Z.X. Xu et al., 2010), as well as in Southeastern China (Zhang et al., 2013; Chi et al., 2013). In contrast, decreasing precipitation was also observed by Qian and Lin (2005) and Liang et al. (2015) in the mid-low Yellow River Basin and the central Yangtze River Basin. However, it should be noted that although no significant overall trends in annual precipitation were detected, considerable spatial disparities in the magnitude of precipitation trends across the three river basins occurred, particularly in the Yangtze River Basin, with a maximum negative trend of −82.03 mm/10a and maximum positive trend of 53.31 mm/10a (Fig. 3B).

In summary, it can be seen that temperature trends in 1957–2013 exhibited differences along the north-to-south axis, whereas the precipitation trends were rather oriented along the southeast–northwest direction. A general warming–wetting tendency was found in the northwestern and southeastern river basins, while the central regions were tending to become warmer and drier during the same period.

3.2.4. Trends in the sub-basins of the three major river basins

The results of our trend analyses presented above (Figs. 3 and 8) also suggest regional differences within each of the three river basins.

The Yellow River Basin showed a remarkable warming trend since 1957, especially in the Upper Basin. Annual mean temperature increased at a rate of up to 0.30 °C/10a, which was the highest warming rate in the whole study area, and the warming rate decreased from the Upper Basin to the Lower Basin along the west–east direction (Table 4). The annual precipitation in the Yellow River Basin slightly decreased mainly in the Middle and Lower basins, but the trend was not statistically significant (Table 4).

The strongest warming in the Yangtze River Basin was detected in the source region (JSJ Basin), but precipitation hardly changed there (Table 4). The multiyear average of annual mean temperature on the North Bank of the Mainstream basin was about 3–5 °C lower than on the South Bank, but both regions showed similar warming rates. The multiyear average of annual precipitation on the North Bank was about 500 mm lower than on the South Bank. Precipitation showed decreases on the North Bank, while heterogeneous trends were found over the South Bank river subbasins (Table 4). The Mainstream subbasin showed a significant warming, but with much higher amplitude in the Mid-Lower Mainstream, while the precipitation hardly changed over the Mainstream subbasin (slightly negative trend in Upper Mainstream, slightly positive trend in Mid-Lower Mainstream) (Table 4).

Climate variations in the Pearl River Basin exhibited a zonal contrast with a significant warming rate in the West River Basin and an even higher rate over the eastern part of the Pearl River Basin since 1957. Precipitation, however, did not change significantly (Table 4).

3.3. Covariation of land temperature and precipitation with SST

Coupled variations of seasonal temperature and precipitation in the three river basins with SST on the interannual time scale were revealed by the MCA method, based on the 7-year high-pass filtered data of seasonal temperature, precipitation and SST since

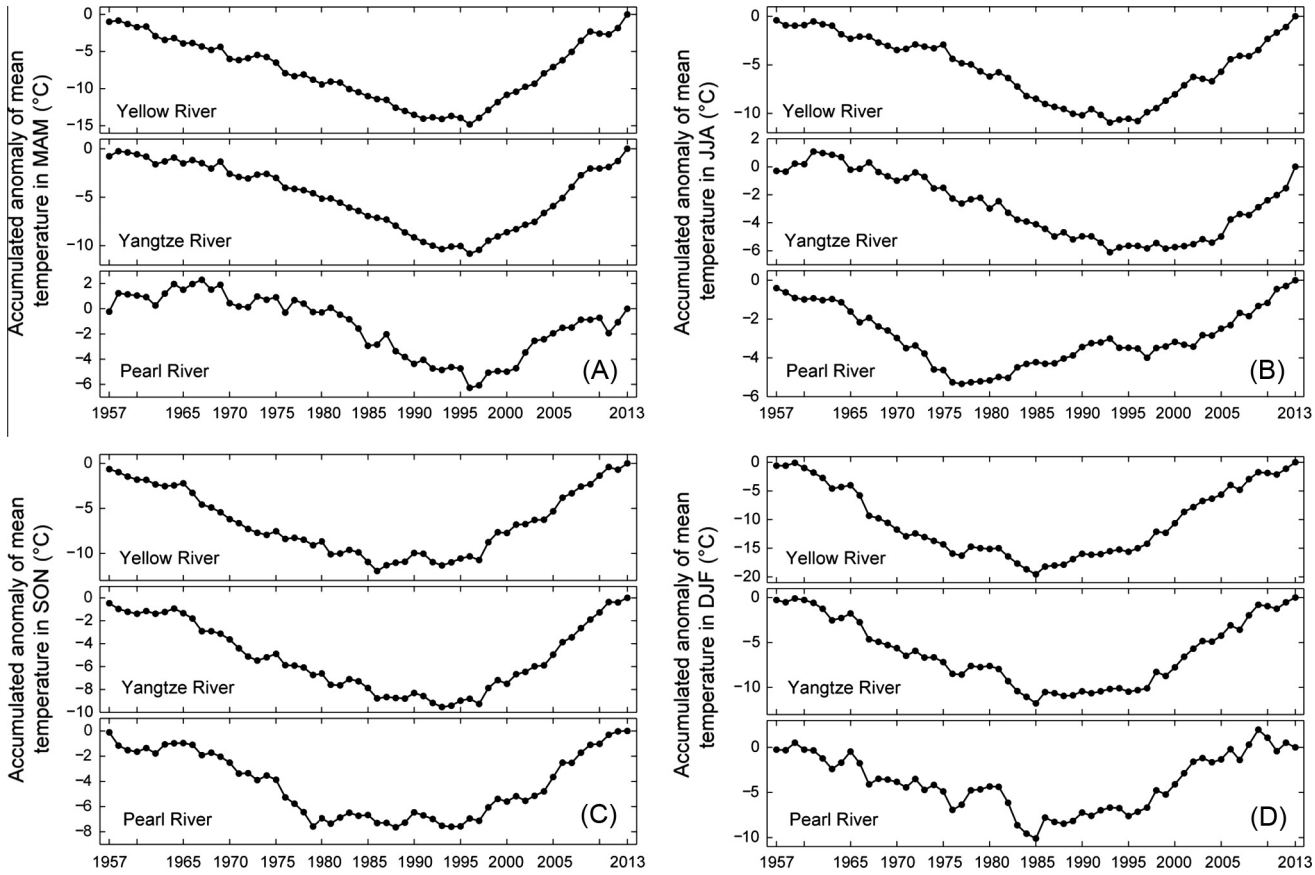

Fig. 9. The Accumulated Anomaly Curves of seasonal mean temperature for MAM (A), JJA (B), SON (C), and DJF (D) in the three river basins. Note the different scaling of *y*-axes.

Table 4
Mann–Kendall test results for trends in annual mean temperature and annual precipitation in the river subbasins.

River	Subbasin	Annual mean temperature				Annual precipitation			
		Multiyear average (°C)	Z_{mk}	β (°C/10a)	H_0	Multiyear average (mm)	Z_{mk}	β (mm/10a)	H_0
Yellow River	UB	4.24	6.38	0.30	R	383.33	0.27	1.31	A
	MB	9.66	4.95	0.24	R	519.40	−1.59	−10.93	A
	LB	12.27	4.40	0.18	R	703.77	−0.82	−11.91	A
Yangtze River	JSJ	6.19	5.42	0.24	R	648.33	1.30	4.89	A
	North Bank								
	MJ	10.42	4.34	0.15	R	959.31	−1.74	−10.60	A
	JLJ	14.22	3.13	0.11	R	872.51	−0.86	−7.23	A
	HJ	14.64	3.64	0.16	R	838.39	−0.34	−4.23	A
	South Bank								
	WJ	15.05	2.88	0.10	R	1125.57	−1.80	−18.76	A
	DL	16.84	3.97	0.14	R	1402.48	−0.21	−13.55	A
	PL	17.80	4.54	0.16	R	1637.69	0.70	17.46	A
	Mainstream								
	UM	16.56	2.72	0.10	R	1107.44	−1.36	−12.51	A
	M-LM	15.92	4.67	0.22	R	1264.08	0.17	2.03	A
Pearl River	WR	19.07	3.35	0.11	R	1392.95	−1.01	−11.94	A
	NR	20.30	3.89	0.12	R	1692.64	0.30	5.99	A
	ER	21.16	4.58	0.15	R	1808.71	−0.12	−1.57	A

1957. Moreover, covariances on the decadal time scale were also analyzed, based on the 7–15 year band-pass filtered data. Our MCA results are presented by means of homogeneous and heterogeneous correlation maps. The homogeneous correlation between the SST at every grid point and the temporal expansion coefficient of the leading SVD mode of SST illustrates the spatial pattern of SST variability associated with this expansion coefficient. In the heterogeneous correlation, the same SST expansion coefficient is correlated with precipitation (land temperature) at every grid point over the major Chinese river basins to indicate the potential for predicting precipitation (land temperature) anomalies in the river basins from the leading expansion coefficient of SST.

3.3.1. Interannual covariation of precipitation and SST

The first coupled mode of precipitation and SST in the spring season (MAM) explained 25.10% of the squared covariance (Table 5) and revealed that precipitation in the Yellow River Basin and Middle–Lower basins of the Yangtze River Basin were positively

correlated with the SST in the central and eastern equatorial Pacific and Indian Ocean, but negatively correlated with the SST in the western tropical Pacific on the interannual time scale (Fig. 10A). This indicates that the Yellow River Basin and Middle–Lower basins of the Yangtze River Basin could have spring flood (drought) in years when the central and eastern tropical Pacific and Indian Ocean were abnormally warm (cold) and the western tropical Pacific was abnormally cold (warm). This pattern of SST variation corresponds to a typical ENSO (El Niño-Southern Oscillation) mode.

The first mode of precipitation and SST in JJA only explained 15.15% of the covariance, but the correlation coefficient between the two principal components (PCs) was 0.71 (Table 5). The heterogeneous correlation pattern showed that the interannual variation of precipitation in JJA over the Middle Yellow River Basin was clearly linked to the variation of SSTs in the central and eastern tropical Pacific Ocean in opposite ways (with La Niña phases causing an increase in precipitation) (Fig. 10B). This is in accordance with previous studies showing that when the central and eastern tropical Pacific was abnormally warm (cold) in JJA, the East Asian summer monsoon circulation tended to be weak (strong) and the monsoon onset was usually delayed (earlier), and thus less (more) precipitation than usual was detected over the northern river basins, while more (less) precipitation was found over the southern river basins (Yang and Lau, 2004; Ye, 2014). For example, the Yellow River dried up for 226 consecutive days due to the El Niño event in 1997 (Xu, 2004) which continued for the first half year of 1998 and thus made the Yangtze River Basin suffer from the worst flood disaster during the last 60 years.

The interannual variation of precipitation in SON over the three river basins was also mostly determined by the ENSO-driven variation of SST, with maximum positive (negative) anomalies in the central and eastern tropical Pacific and Indian Ocean, but opposite anomalies in the western Pacific. When SSTs over the central and eastern tropical Pacific were abnormally high (low) in autumn (SON), less (more) precipitation occurred in the region north of the Mainstream of Yangtze River, while more (less) precipitation was detected in the southern river basins at the same time (Fig. 10C).

In the winter (DJF) season, the first mode explained 48.27% of the SST variance, 51.07% of the precipitation variance and 45.20% of the precipitation–SST covariance (Table 5). In this mode, precipitation in the southeastern part of our study area, was positively correlated with the ENSO SST variations (Fig. 10D). Consequently, warm El Niño (cold La Niña) phases appear to coincide with higher positive (negative) precipitation anomalies throughout the Pearl River Basin, as well as the Poyang Lake and Dongting Lake basins of the Yangtze River.

Overall, the MCA reveals that ENSO SST patterns affected precipitation variability over the major Chinese river basins throughout the year, but with very different spatial response patterns in the different seasons. The Mainstream of Yangtze River could be considered as the dividing line to separate the whole study area into two parts: the southern part was more influenced by SSTs than the northern part, except in summer. Yang and Lau (2004) suggested a physical mechanism that explains the causal links between the interannual variations of precipitation and SST in terms of low- and mid-level tropospheric circulation anomalies in spring and summer.

3.3.2. Interannual covariation of land temperature and SST

The first coupled mode explained 29.24% of SST variance, 35.07% of land temperature variance, and 32.30% of the covariance of land temperature and SST in spring (Table 6). This mode also revealed typical ENSO SST variations, which were positively correlated with the temperature variations in the Pearl River and Yangtze River basins, especially in the southwestern part (Fig. 11A). In JJA, abnormally high (low) SST in the central and eastern tropical Pacific corresponded to a negative (positive) temperature anomaly in the Yangtze River Basin (Fig. 11B). In autumn, abnormally low (high) temperatures in the source regions of Yangtze River located on the Tibet Plateau covaried with unusually high (low) SST in the central and east Pacific and Indian Ocean and with lower (higher) SST in the western tropical Pacific (Fig. 11C). Winter temperatures over most of the river basins (except for the Yangtze and Yellow River source regions) were positively correlated to the ENSO mode of SST variation (Fig. 11D).

Overall, interannually varying summer and autumn mean temperatures over the three river basins were negatively correlated to the ENSO-driven variation of SST during the last 6 decades, while they were positively correlated in winter and spring. Despite the different signs of correlation in different seasons, the covariation of seasonal mean land temperature with SST was spatially much more coherent over the study area than the precipitation patterns discussed above.

3.3.3. Decadal covariation of precipitation and SST

Different from the first SST mode on the interannual time scale, which reflected ENSO, the decadal-scale leading mode showed SST variations that were much more pronounced in the eastern North Pacific (Fig. 12). Compared to ENSO, the SST pattern was less equatorially confined in the eastern Pacific, and SST anomalies mostly stretched from the northeast Pacific to the central equatorial Pacific. This SST pattern is typical for the Pacific Quasi-Decadal Oscillation (QDO) which exhibits warmer conditions in the central and eastern tropical and northeastern Pacific during its warm/positive phase and has been described in previous studies (e.g. Tourre et al., 2001; White and Liu, 2008).

In the first coupled mode on the decadal time scale during the MAM season, SST anomalies in the central and eastern tropical Pacific and Indian Ocean were positively correlated with the precipitation in the southeastern part of the study area (the Pearl River Basin, and Poyang Lake Basin of the Yangtze River), but negatively correlated with the precipitation in the Yellow River and the Hanjiang and Wujiang basins of the Yangtze River (Fig. 12A).

According to the first coupled mode during the summer season, which explained 33.67% of the covariance of precipitation and SST (Table 7), the precipitation in the basins south of the Yangtze River Mainstream and most of the Upper–Middle basins of the Yellow River was higher (lower) when SSTs experienced a warm (cool)

Table 5
Percentage variances of SST, precipitation and the SST–precipitation covariance explained by the leading SVD mode in 1957–2013, and the correlations between the PCs of SST and precipitation modes on the interannual time scale. The last column denotes the 95% confidence interval calculated by Pearson T3 (Olafsdottir and Mudelsee, 2014) for the correlation between the PCs. Pearson T3 takes non-normal distributional shapes and serial correlation of time series into account.

1957–2013		Precipitation variance (%)	SST variance (%)	Precipitation–SST covariance (%)	Correlation (PC-P, PC-SST)	95% confidence interval
MAM	SVD1	22.28	32.65	25.10	0.67	(0.54, 0.77)
JJA	SVD1	7.07	33.05	15.15	0.71	(0.54, 0.83)
SON	SVD1	17.55	52.39	29.35	0.66	(0.47, 0.79)
DJF	SVD1	51.07	48.27	45.20	0.57	(0.32, 0.74)

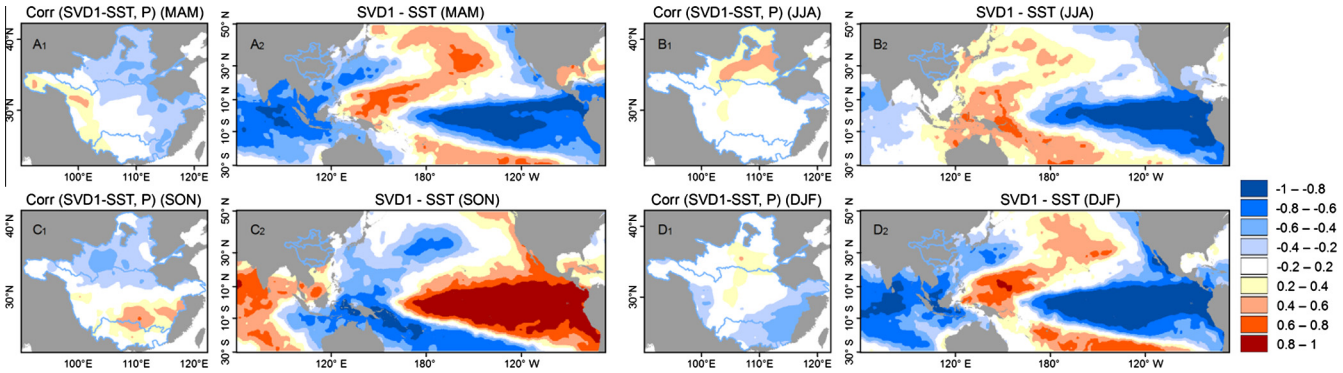

Fig. 10. Heterogeneous correlation of the leading SVD expansion coefficient of SST with precipitation over China (A_1–D_1), and homogeneous correlation of the leading SVD expansion coefficient of SST with SST at every grid point (A_2–D_2). All data entering the analysis have been 7-year high-pass filtered.

Table 6
As Table 5, but for SST and land temperature.

1957–2013		Temperature variance (%)	SST variance (%)	Temperature–SST covariance (%)	Correlation (PC-T, PC-SST)	95% confidence interval
MAM	SVD1	35.07	29.24	32.30	0.57	(0.35, 0.73)
JJA	SVD1	43.25	22.91	27.19	0.51	(0.31, 0.67)
SON	SVD1	18.29	50.02	29.61	0.52	(0.22, 0.73)
DJF	SVD1	62.65	43.35	40.42	0.38	(0.13, 0.58)

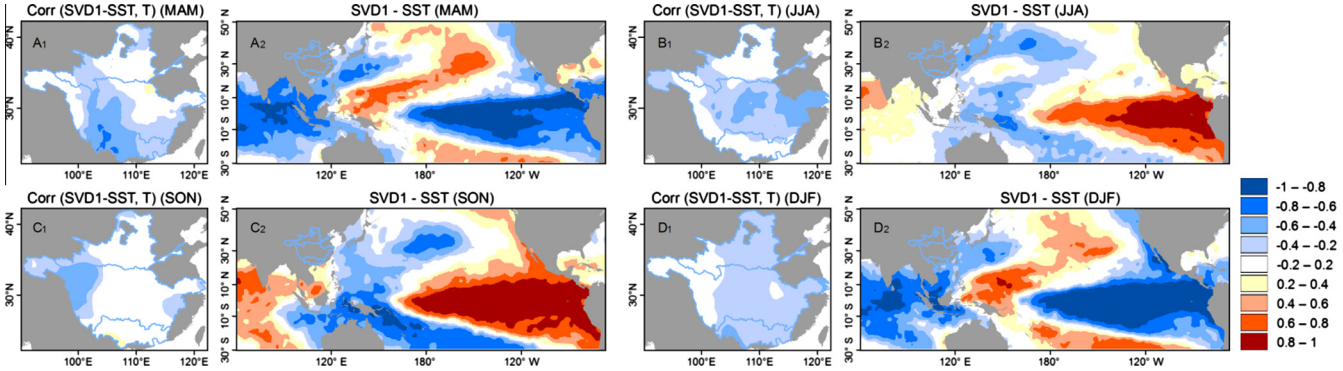

Fig. 11. As Fig. 10, but for land temperature and SST.

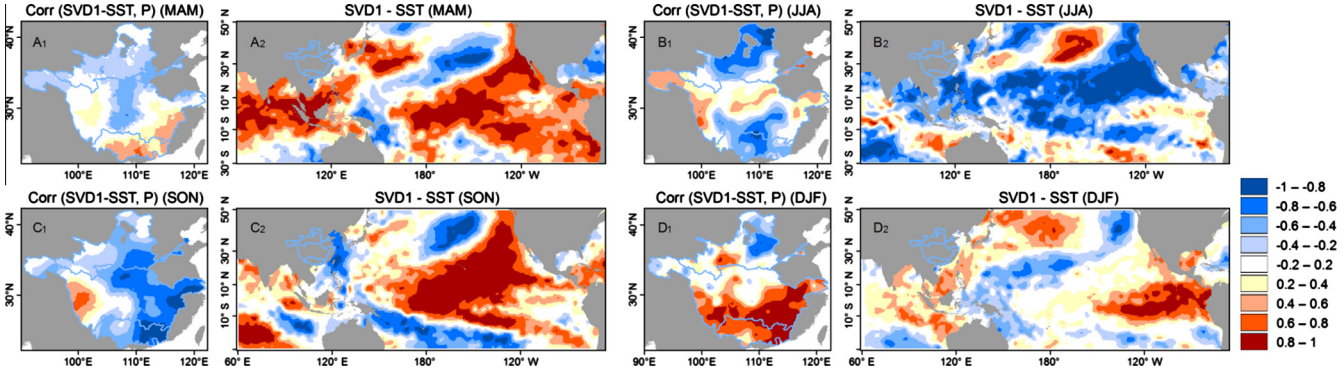

Fig. 12. As Fig. 10, but for the 7–15 year band-pass filtered data.

QDO-like pattern (Fig. 12B). In autumn, 46.92% of the covariance was explained by the first mode, in which a warm (cold) Pacific QDO phase corresponded well with less (more) rain in most areas of the three river basins except for some parts of the JSJ Basin (Fig. 12C). In the first coupled mode during the winter season, precipitation variations in the Middle Basin of the Yellow River were out of phase with the basins south of the Yangtze River Mainstream, with precipitation in these southern regions being positively correlated with tropical eastern Pacific and extratropical North Pacific SST (Fig. 12D).

Table 7
As Table 5, but for the decadal time scale (7–15 year band-pass filter).

1957–2013		Precipitation variance (%)	SST variance (%)	Precipitation–SST covariance (%)	Correlation (PC-P, PC-SST)	95% confidence interval
MAM	SVD1	30.75	38.13	33.69	0.94	(0.71, 0.99)
JJA	SVD1	33.97	33.43	33.67	0.98	(0.86, 1.00)
SON	SVD1	53.23	41.18	46.92	0.98	(0.93, 1.00)
DJF	SVD1	72.01	14.71	41.46	0.95	(0.92, 0.97)

3.3.4. Decadal covariation of land temperature and SST

The (quasi-)decadal covariance of seasonal mean land temperature and SST is shown in Table 8 and Fig. 13. Again, leading modes reveal QDO-like SST patterns (cf. Tourre et al., 2001; White and Liu, 2008) in all the four seasons. The temperature across almost the entire study area was out of phase with the QDO-like mode of SST in spring (Fig. 13A) and autumn (Fig. 13C) (i.e. lower land temperature during the warm Pacific QDO phase), and in phase in summer (Fig. 13B) and winter (Fig. 13D) (i.e. higher land temperature during the warm Pacific QDO phase). In summary, precipitation and temperature anomalies in the three river basins associated with the Pacific QDO pattern of SST showed both similar and different spatial patterns compared to the interannual ENSO mode (Figs. 12 and 13).

4. Perspectives on runoff changes in the three major river basins

An overall decrease in runoff and the subsequent decrease in sediment load of the three rivers since the 1950s have been reported by numerous studies. Runoff reduction induced by natural climate variations was far exceeded by the effects of human activities over the long term (Yang et al., 2010). However, interannual climate variations possibly linked to El Niño/La Niña events may have caused interannual fluctuations of river runoff, and consequent floods and droughts in the river basins. Different opinions still exist on to what extent climate variations can influence the runoff. In this section, we discuss the impact of climate variations on the hydrological factors of the three major river basins.

4.1. Yellow River Basin

The source region above the Tangnaihai hydrological station in the Yellow River contributed about 35% of the annual water discharge (Hu et al., 2011), and the runoff from there was influenced by climate variations, given the fact that the anthropogenic influences in the source region were weak due to the high elevation and harsh climate conditions. The extremely significant warming trend we found in the Upper Basin of the Yellow River all year round since 1957 acted to increase the evaporation (Cuo et al., 2013; Liu and Cui, 2011) as well as the snowmelt water supplement on runoff, especially in spring and summer. However, the contribution of annual snowmelt to runoff was very limited, because rainfall dominated the annual surface runoff in the Upper Basin (Cuo et al., 2013). The slightly increased precipitation since 1957 (Fig. 3B) would have produced more runoff; however the annual runoff from the Upper Basin has decreased (Cuo et al., 2013). Obviously, the loss of runoff due to increasing temperature exceeded the slightly increased precipitation over the Upper Basin.

Rainfall is the primary water source in the middle Yellow River Basin. According to the above analysis, precipitation showed negative trends of various magnitudes across the Middle Basin of the Yellow River since 1957, except for the winter dry season (Figs. 3B and 8E–H, Table 4). Strong evaporation and drought was exacerbated by the significant warming and precipitation reduction overall, and led to severe water scarcity in the Middle Basin of the river basin. This may partly explain increasing numbers of zero-flow days in the Yellow River, especially after the 1980s (Xu, 2004). In addition, 90% of the sediment load from the Yellow River was contributed by the highly erodible area (21.2×10^4 km^2) of the Loess Plateau located in the Middle Basin (CRSB, 2000–2007; Peng et al., 2010), which was primarily attributed to the summer rainfall (Liu et al., 2013). Therefore, the reduction in summer precipitation (Fig. 8F) and extreme rainfall events (Fu et al., 2013) in the Middle Basin should have been the most important climatic cause, responsible for the significant reduction in annual runoff (approximately 7.93% decrease due to climate change in 1950–2009, according to Wang et al. (2012)) and the subsequent reduction of sediment load in the Yellow River since 1957. Climate impacts on runoff in the Lower Basin of the Yellow River could be negligible because of its very small area.

4.2. Yangtze River Basin

Climate warming occurred all year round across the Yangtze River Basin except for some parts in summer (Fig. 8A–D), which may have led to a modest increase of glacier and snowmelt water in the source region. However, evaporation exhibited a significant downward trend due to a significant reduction in net solar radiation and wind speed over several decades (Xu et al., 2006), except

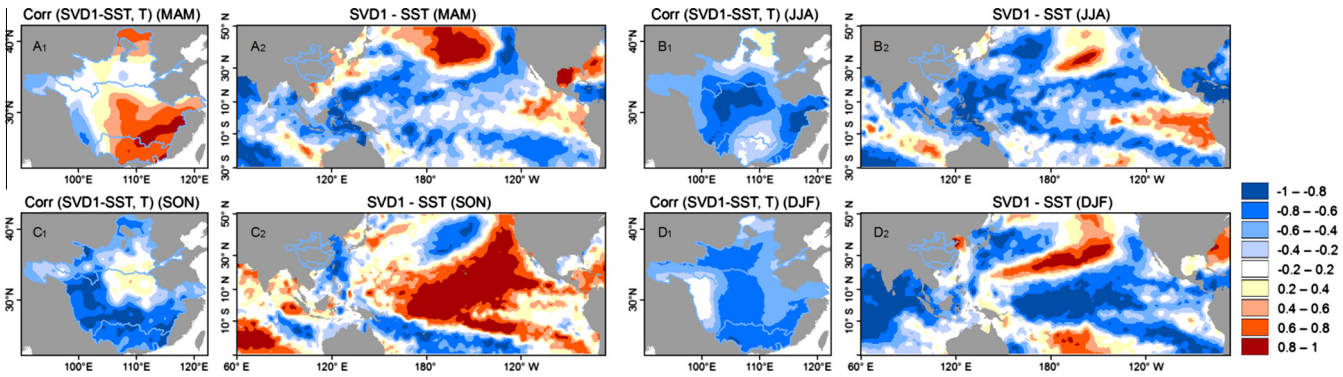

Fig. 13. As Fig. 12, but for land temperature and SST.

Table 8
As Table 7, but for SST and land temperature.

1957–2013		Temperature variance (%)	SST variance (%)	Temperature–SST covariance (%)	Correlation (PC-T, PC-SST)	95% confidence interval
MAM	SVD1	36.96	25.55	31.14	0.87	(0.43, 0.98)
JJA	SVD1	43.31	29.09	36.85	0.93	(0.59, 0.99)
SON	SVD1	48.85	40.05	44.29	0.95	(0.56, 1.00)
DJF	SVD1	78.13	32.26	51.20	0.73	(−0.01, 0.95)

in the JSJ Basin (Y. Wang et al., 2011), the source region of the Yangtze River. Meanwhile, precipitation as the primary water source in the Yangtze River Basin exhibited heterogeneous spatial and seasonal variations over the catchment (Fig. 8E–H). Heterogeneous variations in runoff were observed in the subbasins when all these factors were integrated. For example, the annual runoff of the JSJ Basin showed a slight reduction due to climate change (Sun et al., 2013), while the annual runoff of the Poyang Lake Basin increased over the same period (Ye et al., 2013). The summer precipitation in parts of the eastern plain river basins exhibited a significant increase since 1957 (Fig. 8F), and combined with the flat topography, could easily lead to flood hazard in the Middle–Lower Mainstream.

4.3. Pearl River Basin

Accompanied by the significant reduction in evaporation mainly influenced by the maximum air temperature (Liu et al., 2010), or more cloudy days and aerosol concentration (Zhang et al., 2014) during the last few decades, the precipitation in the Pearl River Basin did not show significant long-term changes as analyzed above (Fig. 8E–H). Only about 10% reduction in runoff and sediment load was contributed by climate change in 1954–2009 in the Pearl River Basin (Wu et al., 2012). However, the year-to-year values of runoff and sediment load of the Pearl River fluctuated with precipitation over the past few decades, while the total amount of runoff and sediment load was significantly reduced overall since the 1950s (Wu et al., 2012; Zhang et al., 2009; H. Wang et al., 2011).

5. Conclusions

The characteristics of annual and seasonal precipitation and temperature variations in the three major Chinese river basins (the Yellow River, Yangtze River and Pearl River) in the period of 1957–2013 were analyzed in this study, as well as their links to variations in SST in the Pacific and Indian Ocean on both interannual and decadal time scales.

The annual mean temperature over the three river basins in general increased significantly since 1957, with the average warming rate of about 0.19 °C/10a in the whole study area. The obvious increase of annual mean temperature was mainly attributed to a significant warming trend in autumn and even higher in the spring and winter season in terms of the warming rate, particularly in the Yellow River Basin and the source region of the Yangtze River Basin. However, the warming process over the three river basins was characterized by an obvious staircase form around 1987 and 1998 over the past 57 years, instead of a monotonic upward trend. Spatially, the warming rates in the northern basins were much higher than in the southern basins overall, and the most significant warming rate was found in the Yellow River Basin and the western source region of the Yangtze River with high altitudes, as well as in the eastern coastal area of the Yangtze River Basin with intense human activities.

However, both the annual precipitation and seasonal mean precipitation in the three river basins showed little long-term change, but exhibited distinct interannual variations during the studied period. Besides, the trend of precipitation showed complex regional differences: a general decrease of annual precipitation was found mostly in the central part of the study area (the Middle–Lower basins of the Yellow River, the central area of the Yangtze River and the West River Basin of the Pearl River), while the annual precipitation in the western source regions of the Yellow River and the Yangtze River located on the Qinghai–Tibetan Plateau, as well as the Middle–Lower basins in the southeastern region has slightly increased since 1957.

The temperature trend showed a pronounced north–south disparity, whereas the trend in precipitation was more distinct along the southeast–northwest direction. Overall, a warming–wetting tendency was found in the northwestern and southeastern river basins during 1957–2013, while the central regions tended to become warmer and drier during the same period.

Interannual variations in precipitation over the three major river basins were associated with ENSO-driven SST variability, but with different characteristics in the different seasons. For example, ENSO patterns of SST variations were positively correlated with the precipitation in the southeastern basins in winter, but negatively correlated with the precipitation over the Yellow River Basin in summer. In autumn, a negative relationship of ENSO SST to the precipitation in the basin north of the Mainstream of the Yangtze River was found, but a positive correlation with the precipitation in the southern river basins. Land temperature variability was also found to be related to the ENSO SST mode, but compared to precipitation, the interannual covariation of seasonal mean land temperature with SST was more spatially homogeneous in the study area in the individual seasons. Temperatures over large portions of the study area were negatively correlated with the ENSO mode of SST variability during the past six decades during summer and autumn, but positively correlated in winter and spring. Our findings thus emphasize the need to distinguish between seasons when studying atmosphere–ocean teleconnections. On decadal time scale, variations in seasonal mean precipitation and land temperature were associated with QDO-like variations in Pacific SST. As such, our results suggest that possible future shifts in the Pacific SST as suggested by climate model scenario runs (e.g. Collins et al., 2010; Taschetto et al., 2014) have the potential to affect seasonal patterns of precipitation and temperature over the major Chinese river basins. Based on our findings on temperature and precipitation changes, this study discussed the possible links of these variations to the runoff/sediment load changes in the three river basins described in previous studies. Using hydrological models (e.g. Vetter et al., 2015) in future studies to investigate the impact of climate variations on hydrological processes in the river basins will provide much stronger conclusions for suitable water resource regulating projects and further insight for predicting the hydrological response to projected global warming.

Acknowledgments

This research was supported through a scholarship by the Deutscher Akademischer Austauschdienst (DAAD), the DFG-Research Center/Cluster of Excellence "The Ocean in the Earth Sys-

tem", and the State Key Laboratory of Estuarine and Coastal Research. Prof. Michael Schulz is thanked for the discussions and helpful suggestions. We thank the anonymous reviewers for their suggestions and comments on an earlier version of the manuscript.

References

Alexander, L.V., Uotila, P., Nicholls, N., 2009. Influence of sea surface temperature variability on global temperature and precipitation extremes. J. Geophys. Res.: Atmos. 114, D18116. http://dx.doi.org/10.1029/2009JD012301.

Bretherton, C.S., Smith, C., Wallace, J.M., 1992. An intercomparison of methods for finding coupled patterns in climate data. J. Climate 5, 541–560. http://dx.doi.org/10.1175/1520-0442(1992) 005<0541:AIOMFF>2.0.CO;2.

Chi, Y., Zhang, C., Liang, C., Wu, H., 2013. The precipitation change in Eastern Forest Regions of China in recent 50 years. Acta Ecol. Sin. 33, 217–226. http://dx.doi.org/10.1016/j.chnaes.2013.05.009.

Chinese River Sediment Bulletin (CRSB), 2000–2007 and 2013. Ministry of Water Resources of China, Beijing, China (in Chinese).

Collins, M., An, S.-I., Cai, W., Ganachaud, A., Guilyardi, E., Jin, F.F., Jochum, M., Lengaigne, M., Power, S., Timmermann, A., Vecchi, G., Wittenberg, A., 2010. The impact of global warming on the tropical Pacific Ocean and El Niño. Nat. Geosci. 3, 391–397. http://dx.doi.org/10.1038/ngeo868.

Cuo, L., Zhang, Y., Gao, Y., Hao, Z., Cairang, L., 2013. The impacts of climate change and land cover/use transition on the hydrology in the upper Yellow River Basin, China. J. Hydrol. 502, 37–52. http://dx.doi.org/10.1016/j.jhydrol.2013.08.003.

Dai, A., Qian, T.T., Trenberth, K.E., Milliman, J.D., 2009. Changes in continental freshwater discharge from 1948 to 2004. J. Climate 22, 2773–2792. http://dx.doi.org/10.1175/2008JCLI2592.1.

Dai, Z., Liu, J.T., Wei, W., Chen, J., 2014. Detection of the Three Gorges Dam influence on the Changjiang (Yangtze River) submerged delta. Sci. Rep. 4, 1–7. http://dx.doi.org/10.1038/srep06600.

Fu, G., Yu, J., Yu, X., Ouyang, R., Zhang, Y., Wang, P., Liu, W., Min, L., 2013. Temporal variation of extreme rainfall events in China, 1961–2009. J. Hydrol. 487, 48–59. http://dx.doi.org/10.1016/j.jhydrol.2013.02.021.

Gardner, L.R., 2009. Assessing the effect of climate change on mean annual runoff. J. Hydrol. 379, 351–359. http://dx.doi.org/10.1016/j.jhydrol.2009.10.021.

Gerten, D., Rost, S., von Bloh, W., Lucht, W., 2008. Causes of change in 20th century global river discharge. Geophys. Res. Lett. 35, L20405. http://dx.doi.org/10.1029/2008GL035258.

Hao, X.M., Chen, Y.N., Xu, C.C., Li, W., 2008. Impacts of climate change and human activities on the Surface runoff in the Tarim River basin over the last fifty years. Water Resour. Manage. 22, 1159–1171. http://dx.doi.org/10.1007/s11269-007-9218-4.

Hartmann, H., Becker, S., King, L., 2008. Predicting summer rainfall in the Yangtze River basin with neural networks. Int. J. Climatol. 28, 925–936. http://dx.doi.org/10.1002/joc.1588.

Hoan, L.X., Hanson, H., Larson, M., Nam, P.T., 2011. Modeling regional sediment transport and shoreline response in the vicinity of tidal inlets on the Long Island coast, United States. Coast. Eng. 58, 554–561. http://dx.doi.org/10.1016/j.coastaleng.2011.03.003.

Hu, Y., Maskey, S., Uhlenbrook, S., Zhao, H., 2011. Streamflow trends and climate linkages in the source region of the Yellow River, China. Hydrol. Process. 25, 3399–3411. http://dx.doi.org/10.1002/hyp.8069.

Hu, Z.Z., Yang, S., Wu, R., 2003. Long-term climate variations in China and global warming signals. J. Geophys. Res. D: Atmos. 108 (19). http://dx.doi.org/10.1029/2003JD003651. ACL 11-1–ACL 11-13.

IPCC AR5, 2013. In: Stocker, T.F., Qin, D., Plattner, G.K., Tignor, M., Allen, S.K., Boschung, J., Nauels, A., Xia, Y., Bex, V., Midgley, P.M. (Eds.), Climate Change 2013: The Physical Science Basis. Contribution of Working Group I to the Fifth Assessment Report of the Intergovernmental Panel on Climate Change. Cambridge University Press, Cambridge, United Kingdom and New York, NY, USA, 1535 pp.

Jones, P.D., Lister, D.H., Osborn, T.J., Harpham, C., Salmon, M., Morice, C.P., 2012. Hemispheric and large-scale land surface air temperature variations: an extensive revision and an update to 2010. J. Geophys. Res. 117, D05127. http://dx.doi.org/10.1029/2011JD017139.

Kam, J., Sheffield, J., Yuan, X., Wood, E.F., 2014. Did a skillful prediction of sea surface temperatures help or hinder forecasting of the 2012 Midwestern US drought? Environ. Res. Lett. 9, 034005. http://dx.doi.org/10.1088/1748-9326/9/3/034005.

Kendall, M.G., 1975. Rank Correlation Methods. Griffin, London.

Kenyon, J., Hegerl, G.C., 2008. Influence of modes of climate variability on global temperature extremes. J. Climate 21, 3872–3889. http://dx.doi.org/10.1175/2008JCLI2125.1.

Kenyon, J., Hegerl, G.C., 2010. Influence of modes of climate variability on global precipitation extremes. J. Climate 23, 6248–6262. http://dx.doi.org/10.1175/2010JCLI3617.1.

Krige, D.G., 1951. A Statistical Approach to Some Mine Valuations and Allied Problems at the Witwatersrand. Master's thesis of the University of Witwatersrand.

Kumar, K.K., Rajagopalan, B., Hoerling, M., Bates, G., Cane, M., 2006. Unraveling the mystery of Indian monsoon failure during El Niño. Science 314, 115–119. http://dx.doi.org/10.1126/science.1131152.

Lamberth, S.J., Drapeau, L., Branch, G.M., 2009. The effects of altered freshwater inflows on catch rates of non-estuarine-dependent fish in a multispecies nearshore linefishery. Estuar. Coast. Shelf Sci. 84, 527–538. http://dx.doi.org/10.1016/j.ecss.2009.07.021.

Lau, K.M., Wu, H.T., 2001. Principal modes of rainfall-SST variability of the Asian summer monsoon: a reassessment of the monsoon–ENSO relationship. J. Climate 14 (13), 2880–2895.

Legesse, D., Abiye, T.A., Vallet-Coulomb, C., Abate, H., 2010. Streamflow sensitivity to climate and land cover changes: Meki River, Ethiopia. Hydrol. Earth Syst. Sci. 14, 2277–2287. http://dx.doi.org/10.5194/hess-14-2277-2010.

Li, H., Dai, A., Zhou, T., Lu, J., 2010. Responses of East Asian summer monsoon to historical SST and atmospheric forcing during 1950–2000. Clim. Dyn. 34, 501–514. http://dx.doi.org/10.1007/s00382-008-0482-7.

Li, Z., He, Y., Wang, P., Theakstone, W.H., An, W., Wang, X., Lu, A., Zhang, W., Cao, W., 2012. Changes of daily climate extremes in southwestern China during 1961–2008. Global Planet. Change 80–81, 255–272. http://dx.doi.org/10.1016/j.gloplacha.2011.06.008.

Liang, K., Liu, S., Bai, P., Nie, R., 2015. The Yellow River basin becomes wetter or drier? The case as indicated by mean precipitation and extremes during 1961–2012. Theor. Appl. Climatol. 119, 701–722. http://dx.doi.org/10.1007/s00704-014-1138-7.

Liu, J., Wang, G., Li, H., Gong, J., Han, J., 2013. Water and sediment evolution in areas with high and coarse sediment yield of the Loess Plateau. Int. J. Sedim. Res. 28, 448–457. http://dx.doi.org/10.1016/S1001-6279(14)60004-4.

Liu, M., Tian, H., Lu, C., Xu, X., Chen, G., Ren, W., 2012. Effects of multiple environment stresses on evapotranspiration and runoff over eastern China. J. Hydrol. 426–427, 39–54. http://dx.doi.org/10.1016/j.jhydrol.2012.01.009.

Liu, Q., Cui, B., 2011. Impacts of climate change/variability on the stream flow in the Yellow River Basin, China. Ecol. Model. 222, 268–274. http://dx.doi.org/10.1016/j.ecolmodel.2009.11.022.

Liu, Q., Yang, Z., Xia, X., 2010. Trends for pan evaporation during 1959–2000 in China. Procedia Environ. Sci. 2, 1934–1941. http://dx.doi.org/10.1016/j.proenv.2010.10.206.

Liu, X., Ren, Z., 2005. Progress in quality control of surface meteorological data. Meteorol. Sci. Technol. 33, 199–203.

Lu, X.X., 2004. Vulnerability of water discharge of large Chinese rivers to environmental changes: an overview. Reg. Environ. Change 4, 182–191. http://dx.doi.org/10.1007/s10113-004-0080-0.

Ma, S., Zhou, T., Dai, A., Han, Z., 2015. Observed changes in the distributions of daily precipitation frequency and amount over China from 1960 to 2013. J. Climate 28, 6960–6978. http://dx.doi.org/10.1175/JCLI-D-15-0011.1.

Mann, H.B., 1945. Nonparametric tests against trend. Econometrica 13, 245–259.

Matheron, G., 1973. The intrinsic random functions, and their applications. Adv. Appl. Probab. 5, 439–468.

Meybeck, M., Vörösmarty, C., 2005. Fluvial filtering of land-to-ocean fluxes: from natural Holocene variations to Anthropocene. C. R. Geosci. 337, 107–123.

Miyakoda, K., Navarra, A., Ward, M.N., 2007. Tropical-wide teleconnection and oscillation. II: The enso-monsoon system. Quart. J. Roy. Meteorol. Soc. 125 (560), 2937–2963.

Olafsdottir, K.B., Mudelsee, M., 2014. More accurate, calibrated bootstrap confidence intervals for estimating the correlation between two time series. Math. Geosci. 46, 411–427. http://dx.doi.org/10.1007/s11004-014-9523-4.

Park, T., Jang, C.J., Jungclaus, J.H., Haak, H., Park, W., Oh, I.S., 2011. Effects of the Changjiang river discharge on sea surface warming in the Yellow and East China Seas in summer. Cont. Shelf Res. 31, 15–22. http://dx.doi.org/10.1016/j.csr.2010.10.012.

Peng, J., Chen, S., Dong, P., 2010. Temporal variation of sediment load in the Yellow River basin, China, and its impacts on the lower reaches and the river delta. Catena 83, 135–147. http://dx.doi.org/10.1016/j.catena.2010.08.006.

Qian, W., Lin, X., 2005. Regional trends in recent precipitation indices in China. Meteorol. Atmos. Phys. 90, 193–207. http://dx.doi.org/10.1007/s00703-004-0101-z.

Rayner, N.A., Parker, D.E., Horton, E.B., Folland, C.K., Alexander, L.V., Rowell, D.P., Kent, E.C., Kaplan, A., 2003. Global analyses of sea surface temperature, sea ice, and night marine air temperature since the late nineteenth century. J. Geophys. Res. 108 (D14), 4407. http://dx.doi.org/10.1029/2002JD002670.

Ren, G.Y., Guan, Z.Y., Shao, X.M., Gong, D.Y., 2011. Changes in climatic extremes over mainland China. Climate Res. 50, 105–111. http://dx.doi.org/10.3354/cr01067.

Shi, C., Zhou, Y., Fan, X., Shao, W., 2012. A study on the annual runoff change and its relationship with water and soil conservation practices and climate change in the middle Yellow River basin. Catena 100, 31–41. http://dx.doi.org/10.1016/j.catena.2012.08.007.

Song, C., Huang, B., Ke, L., Keith, S.R., 2014. Seasonal and abrupt changes in the water level of closed lakes on the Tibetan Plateau and implications for climate impacts. J. Hydrol. 514, 131–144. http://dx.doi.org/10.1016/j.jhydrol.2014.04.018.

Sun, J., Lei, X., Tian, Y., Liao, W., Wang, Y., 2013. Hydrological impacts of climate change in the upper reaches of the Yangtze River Basin. Quatern. Int. 304, 62–74. http://dx.doi.org/10.1016/j.quaint.2013.02.038.

Taschetto, A.S., Gupta, A.S., Jourdain, N.C., Santoso, A., Ummenhofer, C.C., England, M.H., 2014. Cold tongue and warm pool ENSO events in CMIP5: mean state and future projections. J. Climate 27, 2861–2885. http://dx.doi.org/10.1175/JCLI-D-13-00437.1.

Tourre, Y.M., Rajagopalan, B., Kushnir, Y., Barlow, M., White, W.B., 2001. Patterns of coherent decadal and interdecadal climate signals in the Pacific basin during the 20th century. Geophys. Res. Lett. 28, 2069–2072. http://dx.doi.org/10.1029/2000GL012780.

Trenberth, K.E., Fasullo, J.T., Mackaro, J., 2011. Atmospheric moisture transports from ocean to land and global energy flows in reanalyses. J. Climate 24, 4907–4924. http://dx.doi.org/10.1175/2011JCLI4171.1.

Vetter, T., Huang, S., Aich, V., Yang, T., Wang, X., Krysanova, V., Hattermann, F., 2015. Multi-model climate impact assessment and intercomparison for three large-scale river basins on three continents. Earth Syst. Dyn. 6, 17–43. http://dx.doi.org/10.5194/esd-6-17-2015.

Wagener, T., Liu, Y., Gupta, H.V., Spinger, E., Brookshire, D. (Eds.), 2005. Regional Hydrological Impacts of Climatic Change: Impact assessment and Decision Making. IAHS Press, Centre for Ecology and Hydrology, UK, p. 163.

Wallace, J.M., Smith, C., Bretherton, C.S., 1992. Singular value decomposition of wintertime sea surface temperature and 500 mb height anomalies. J. Climate 5, 561–576.

Walling, D.E., Fang, D., 2003. Recent trends in the suspended sediment loads of the world's rivers. Global Planet. Change 39, 111–126. http://dx.doi.org/10.1016/S0921-8181(03)00020-1.

Wang, B., Wu, R., Fu, X., 2000. Pacific–East Asian teleconnection: how does ENSO affect East Asian climate. J. Climate 13, 1517–1536. http://dx.doi.org/10.1175/1520-0442.

Wang, F., Yang, S., Higgins, W., Li, Q., Zuo, Z., 2014. Long-term changes in total and extreme precipitation over China and the United States and their links to oceanic–atmospheric features. Int. J. Climatol. 34, 286–302. http://dx.doi.org/10.1002/joc.3685.

Wang, G., Cheng, G., 2000. The characteristic of water resources and the changes of the hydrological process and environment in the arid zone of northwest China. Environ. Geol. 37, 783–790. http://dx.doi.org/10.1007/s002540050494.

Wang, H., Bi, N., Yoshiki, S., Wang, Y., Sun, X., Hu, B., 2010. Recent changes in sediment delivery by the Huanghe (Yellow River) to the sea: causes and environmental implications in its estuary. J. Hydrol. 39 (3–4), 302–313. http://dx.doi.org/10.1016/j.jhydrol.2010.07.030.

Wang, H., Saito, Y., Zhang, Y., Bi, N., Sun, X., Yang, Z., 2011. Recent changes of sediment flux to the western Pacific Ocean from major rivers in East and Southeast Asia. Earth Sci. Rev. 108, 80–100. http://dx.doi.org/10.1016/j.earscirev.2011.06.003.

Wang, S., Yan, M., Yan, Y., Shi, C., He, L., 2012. Contributions of climate change and human activities to the changes in runoff increment in different sections of the Yellow River. Quatern. Int. 282, 66–77. http://dx.doi.org/10.1016/j.quaint.2012.07.011.

Wang, Y., Liu, B., Su, B., Zhai, J., Gemmer, M., 2011. Trends of calculated and simulated actual evaporation in the Yangtze River basin. J. Climate 24, 4494–4507. http://dx.doi.org/10.1175/2011JCLI3933.1.

White, W.B., Liu, Z., 2008. Resonant excitation of the quasi-decadal oscillation by the 11-year signal in the Sun's irradiance. J. Geophys. Res. 113, C01002. http://dx.doi.org/10.1029/2006JC004057.

Wu, C.S., Yang, S.L., Lei, Y., 2012. Quantifying the anthropogenic and climatic impacts on water discharge and sediment load in the Pearl River (Zhujiang), China (1954–2009). J. Hydrol. 452–453, 190–204. http://dx.doi.org/10.1016/j.jhydrol.05.064.

Xu, C., Gong, L., Jiang, T., Chen, D., Singh, V.P., 2006. Analysis of spatial distribution and temporal trend of reference evapotranspiration and pan evaporation in Changjiang (Yangtze River) catchment. J. Hydrol. 327, 81–93. http://dx.doi.org/10.1016/j.jhydrol.2005.11.029.

Xu, J., 2004. A study of anthropogenic seasonal rivers in China. Catena 55, 17–32. http://dx.doi.org/10.1016/S0341-8162(03)00089-4.

Xu, K.H., Milliman, J.D., Xu, H., 2010. Temporal trend of precipitation and runoff in major Chinese Rivers since 1951. Global Planet. Change 73, 219–232. http://dx.doi.org/10.1016/j.gloplacha.2010.07.002.

Xu, Z.X., Liu, Z.F., Fu, G.B., Chen, Y.N., 2010. Hydro-climate trends of the Tarim River Basin for the last 50 years. J. Arid Environ. 74, 256–267.

Yang, F., Lau, K.M., 2004. Trend and variability of China precipitation in spring and summer: linkage to sea-surface temperatures. Int. J. Climatol. 24, 1625–1644. http://dx.doi.org/10.1002/joc.1094.

Yang, S.L., Liu, Z., Dai, S.B., Gao, Z.X., Zhang, J., Wang, H.J., Luo, X.X., Wu, C.S., Zhang, Z., 2010. Temporal variations in water resources in the Yangtze River (Changjiang) over the Industrial Period based on reconstruction of missing monthly discharges. Water Resour. Res. 46, 1–13. http://dx.doi.org/10.1029/2009WR008589.

Yang, S.L., Milliman, J.D., Xu, K.H., Deng, B., Zhang, X.Y., Luo, X.X., 2014. Downstream sedimentary and geomorphic impacts of the Three Gorges Dam on the Yangtze River. Earth Sci. Rev. 138, 469–486. http://dx.doi.org/10.1016/j.earscirev.2014.0 7.006.

Ye, J., Li, F., Sun, G., Guo, A., 2010. Solar dimming and its impact on estimating solar radiation from diurnal temperature range in China, 1961–2007. Theoret. Appl. Climatol. 101, 137–142. http://dx.doi.org/10.1007/s00704-009-0213-y.

Ye, J.S., 2014. Trend and variability of China's summer precipitation during 1955–2008. Int. J. Climatol. 34, 559–566. http://dx.doi.org/10.1002/joc.3705.

Ye, X., Zhang, Q., Liu, J., Li, X., Xu, C., 2013. Distinguishing the relative impacts of climate change and human activities on variation of streamflow in the Poyang Lake catchment, China. J. Hydrol. 494, 83–95. http://dx.doi.org/10.1016/j.jhydrol.2013.04.036.

Yu, M., Li, Q., Hayes, M.J., Svobodab, M.D., Heim, R.R., 2014. Are droughts becoming more frequent or severe in China based on the Standardized Precipitation Evapotranspiration Index: 1951–2010? Int. J. Climatol. 34, 545–558. http://dx.doi.org/10.1002/joc.3701.

Zhai, P., Zhang, X., Wan, H., Pan, X., 2005. Trends in total precipitation and frequency of daily precipitation extremes over China. J. Climate 18, 1096–1108. http://dx.doi.org/10.1175/JCLI-3318.1.

Zhang, Q., Li, J., Singh, V.P., Xiao, M., 2013. Spatio-temporal relations between temperature and precipitation regimes: implications for temperature-induced changes in the hydrological cycle. Global Planet. Change 111, 57–76. http://dx.doi.org/10.1016/j.gloplacha.2013.08.012.

Zhang, Q., Qi, T.Y., Li, J.F., Singh, V.P., Wang, Z., 2014. Spatiotemporal variations of pan evaporation in China during 1960–2005: changing patterns and causes. Int. J. Climatol. http://dx.doi.org/10.1002/joc.4025.

Zhang, Q., Xu, C.Y., Chen, Y.D., Jiang, J., 2009. Abrupt behaviors of the streamflow of the Pearl River basin and implications for hydrological alterations across the Pearl River Delta, China. J. Hydrol. 377, 274–283. http://dx.doi.org/10.1016/j.jhydrol.2009.08.026.

Zhou, L.T., Huang, R.H., 2010. Interdecadal variability of summer rainfall in Northwest China and its possible causes. Int. J. Climatol. 30, 549–557. http://dx.doi.org/10.1002/joc.1923.